Lee Jinsu (Orcid ID: 0000-0003-3825-288X)
Kim SangGyu (Orcid ID: 0000-0003-2574-3233)
Lee Yuree (Orcid ID: 0000-0002-4663-6974)

MSD2-mediated ROS metabolism fine-tunes the timing of floral organ abscission in Arabidopsis

Jinsu Lee[1,2], Huize Chen[1,3], Gisuk Lee[4], Aurélia Emonet[5], Sang-Gyu Kim[4], Donghwan Shim[6], and Yuree Lee[2,7,8]

[1]Research Institute of Basic Sciences, Seoul National University, Seoul 08826, Republic of Korea; [2]Research Center for Plant Plasticity, Seoul National University, Seoul 08826, Republic of Korea; [3]Higher Education Key Laboratory of Plant Molecular and Environmental Stress Response in Shanxi Province, Shanxi Normal University, Taiyuan, 030000, Shanxi, P. R. China; [4]Department of Biological Sciences, Korea Advanced Institute for Science and Technology, Daejeon 34141, Republic of Korea; [5]Department of Plant Molecular Biology, University of Lausanne, Biophore Building, UNIL-Sorge, 1015 Lausanne, Switzerland; [6]Department of Biological Sciences, Chungnam National University, Daejeon, 34134, Republic of Korea; [7]School of Biological Sciences, Seoul National University, Seoul 08826, Republic of Korea; [8]Plant Genomics and Breeding Institute, Seoul National University, Seoul 08826, Republic of Korea

ORCID:

Jinsu Lee: 0000-0003-3825-288X

Yuree Lee: 0000-0002-4663-6974

Author for correspondence:

Yuree Lee

Tel: +82 2 8802136

Email: yuree.lee@snu.ac.kr

Received: 8 December 2021

Accepted: 27 May 2022

Summary

- The timely removal of end-of-purpose flowering organs is as essential for reproduction and plant survival as timely flowering. Despite much progress in understanding the molecular mechanisms of floral organ abscission, little is known about how various environmental factors are integrated into developmental programs that determine the timing of abscission.
- Here, we investigated whether reactive oxygen species (ROS), mediators of various stress-related signalling pathways, are involved in determining the timing of abscission and, if so, how they are integrated with the developmental pathway in *Arabidopsis thaliana*.
- *MSD2*, encoding a secretory manganese superoxide dismutase, was preferentially expressed in the abscission zone of flowers, and floral organ abscission was accelerated by the accumulation of ROS in *msd2* mutants. The expression of the genes encoding the receptor-like kinase HAESA (HAE) and its cognate peptide ligand INFLORESCENCE DEFICIENT IN ABSCISSION (IDA), the key signalling components of abscission, was accelerated in *msd2* mutants, suggesting that MSD2 acts upstream of IDA-HAE. Further transcriptome and pharmacological analyses revealed that abscisic acid and nitric oxide facilitate abscission by regulating the expression of *IDA* and *HAE* during MSD2-mediated signalling.
- These results suggest that MSD2-dependent ROS metabolism is an important regulatory point integrating environmental stimuli into the developmental program leading to abscission.

Keywords

Arabidopsis thaliana, abscisic acid (ABA), HAESA, MSD2, nitric oxide (NO), Organ abscission, reactive oxygen species (ROS), superoxide dismutases (SOD).

Introduction

Abscission is the natural shedding of plant tissues such as leaves, flowers, seed pods, and fruits and plays an essential role in plant survival as a means of seed dispersal or removal of vulnerable or diseased tissues (Addicott, 1982). The specialised cell layers responsible for abscission are called abscission zones (AZs) and are usually formed together in early stages of organogenesis. When abscission is activated, cell wall–hydrolysing enzymes are secreted to disrupt the cell wall at the AZ in a highly coordinated process that integrates various developmental and environmental cues (Patharkar & Walker, 2019).

The molecular mechanism of abscission has been largely elucidated for the floral organs of Arabidopsis (*Arabidopsis thaliana*) (Cho *et al.*, 2008; Mckim *et al.*, 2008; Liu *et al.*, 2013; Lee *et al.*, 2018). As constituents of reproductive organs, petals play an important role in attracting pollinators but are also easily exposed to predators and are vulnerable to environmental stress, making their timely removal after fertilisation critical for plant survival. Various phytohormones, including ethylene, auxin, abscisic acid (ABA), and jasmonic acid (JA), are involved in activating abscission after fertilisation has occurred (Patterson & Bleecker, 2004; Kim *et al.*, 2013; Meir *et al.*, 2019). The receptor-like kinases HAESA (HAE) and HAE-LIKE2 (HSL2) and their cognate peptide ligand INFLORESCENCE DEFICIENT IN ABSCISSION (IDA) initiate the signalling pathway controlling the expression of genes encoding cell wall enzymes (Cho *et al.*, 2008; Stenvik *et al.*, 2008; Aalen *et al.*, 2013; Patharkar & Walker, 2015). HAE/HSL2 work with the other receptor-like proteins SOMATIC EMBRYOGENESIS RECEPTOR-LIKE KINASEs (SERKs), including SERK1–4, to form complexes upon interaction with IDA to initiate floral abscission (Meng *et al.*, 2016). The IDA-HAE pathway is conserved in various crop species such as tomato (*Solanum lycopersicum*), soybean (*Glycine max*), and tobacco (*Nicotiana tabacum*) and is involved in organ abscission (Tucker & Yang, 2012; Ventimilla *et al.*, 2020; Ventimilla *et al.*, 2021). However, the IDA-HAE module is not limited to floral organ abscission, as it also participates in other cell separation processes such as lateral root emergence and root cap detachment (Kumpf *et al.*, 2013; Shi *et al.*, 2018). Additionally, the expression levels of *IDA* and *IDA-LIKE* (*IDL*) increase in response to abiotic and biotic stress conditions (Vie *et al.*, 2015), suggesting that the IDA-HAE module plays a role in linking stress responses to development. However, how various environmental stimuli modulate IDA-HAE activity is not well understood.

Redox homeostasis plays critical roles in plant development and stress responses

(Mhamdi & Van Breusegem, 2018; Huang *et al.*, 2019). Reactive oxygen species (ROS) are by-products of various cellular processes, including photosynthesis and mitochondrial respiration, in different intracellular compartments. Plants have not only developed various systems for detoxifying ROS but also evolved mechanisms that can integrate ROS as signalling molecules, thus linking metabolism and responses to highly variable environments (Waszczak *et al.*, 2018). ROS accumulation in the AZ has been reported in various species, including Arabidopsis, with roles in abscission signalling and cell wall remodelling (Sakamoto *et al.*, 2008a; Sakamoto *et al.*, 2008b; Bar-Dror *et al.*, 2011; Yang *et al.*, 2015; Liao *et al.*, 2016; Lee *et al.*, 2018). Various enzymes, such as NADPH oxidases, peroxidases, and polyamine oxidases, might be involved in ROS production in the AZ, but how their roles are interconnected and regulated is not clear.

NADPH oxidases located at the cell membrane generate superoxide that might be used as a signal in various developmental and stress conditions (Mittler *et al.*, 2011; Huang *et al.*, 2019). The Arabidopsis genome harbours 10 genes, *RbohA–RbohJ* (*RESPIRATORY BURST OXIDASE HOMOLOG*), encoding NADPH oxidases with functions in various developmental stages, including root and hypocotyl elongation, root hair development, fruit ripening, and cell wall remodelling during seed germination (Dunand *et al.*, 2007; Muller *et al.*, 2009; Yan *et al.*, 2016). *RbohD* and *RbohF* are highly expressed in the AZ and provide the ROS substrates needed for peroxidase-dependent lignin formation, which forms a physical apoplastic barrier to precisely control the localization of cell wall enzymes (Lee *et al.*, 2018). However, it remains unknown whether RBOHs are also involved in signalling to regulate the timing of abscission or cell wall loosening. How the generated ROS are metabolised is also unknown.

Extracellular superoxides ($O2^{\cdot-}$) produced by NADPH oxidases can be dismutated to hydrogen peroxide (H_2O_2) either spontaneously or enzymatically via apoplastic superoxide dismutases (SODs) and transported to the cytoplasm via aquaporins (Qi *et al.*, 2017; Mhamdi & Van Breusegem, 2018). SODs can be divided into three classes as a function of the metal ions in their active centres: manganese (Mn), iron (Fe), and copper and zinc (Cu/Zn). Arabidopsis has eight known SODs: three Cu/Zn SODs (CSD1–3), three Fe SODs (FSD1–3), and two Mn SODs (MSD1–2) (Kliebenstein *et al.*, 1998; Chen *et al.*, 2022). Their subcellular localisations vary, with CSD2 and FSD1–3 in chloroplasts (Kliebenstein *et al.*, 1998; Myouga *et al.*, 2008; Dvorak *et al.*, 2021), MSD1 in mitochondria (Morgan *et al.*, 2008), CSD3 in peroxisomes (Kliebenstein *et al.*, 1998; Huang *et al.*, 2012), CSD1 and FSD1 in the cytoplasm

(Kliebenstein *et al.*, 1998; Dvorak *et al.*, 2021), and FSD1 in the nucleus (Dvorak *et al.*, 2021). MSD2 is an apoplastic SOD with Mn SOD activity that is secreted into vacuoles or the apoplast (Chen *et al.*, 2022). SODs, which convert $O2^{\cdot-}$ into H_2O_2, not only detoxify $O2^{\cdot-}$ accumulated from various stress conditions and metabolic processes, but also affect the redox balance. Given the recent reports that different types of ROS perform distinct functions (Tsukagoshi *et al.*, 2010; Lee *et al.*, 2018), the role of SOD in influencing the balance between $O2^{\cdot-}$ and H_2O_2 may serve as an important signalling rheostat along with ROS-generating enzymes. Although several factors regulating the expression of *SOD*s and the function of the encoded enzymes have recently been identified (Yamasaki *et al.*, 2007; Xing *et al.*, 2013; Dvorak *et al.*, 2020; Hu *et al.*, 2021), our understanding of their regulatory mechanisms and their relationship with other signalling pathways is still fragmentary.

In this study, we demonstrated that MSD2, a recently identified secretory SOD (Chen *et al.*, 2022), is involved in the regulation of abscission signalling. *MSD2* was preferentially expressed in the AZ of flowers, and the encoded MSD2 enzyme was secreted into the vacuole and extracellular spaces. In *msd2* mutants, superoxide accumulated earlier than in the wild type and was accompanied by an acceleration of floral organ shedding. Transcriptome analysis revealed that the expression of nitric oxide (NO)- and ABA-related genes is upregulated in *msd2* mutants. NO and ABA abundance increased upon activation of abscission, and an exogenous supply of NO and ABA accelerated abscission, while treating plants with an NO scavenger blocked the accelerated abscission observed in *msd2* mutants. We also established that the expression of *IDA* and *HAE* is affected by NO and ABA. These results suggest that the regulation of ROS metabolism by MSD2 affects the onset of abscission through the NO and ABA signalling pathways upstream of IDA-HAE.

Materials and Methods

Plant materials and growth conditions

For all experiments, 7-week-old *Arabidopsis thaliana* (accession Col-0) plants were used. After stratification for 2 days (at 4°C in the dark), seeds were sown on a soil:sand mixture (4:1, w/w) and cultivated in a climate chamber with 60% relative humidity under long-day conditions (16-h-light/8-h-dark cycles, 22°C day/18°C night regime, 70 µmol m^{-2} s^{-1} photon flux density). The *ida* and *hae-1 hsl2-1* mutants were described before (Lee *et al.*, 2018). *Msd2*-

1 (GABI_100H05), *msd2-2* (SM_3_35975), *UBQ10pro:MSD2-mCherry*, and *MSD2pro:nlsGFP-GUS* were described by Chen *et al*. (2022).

NO, cPTIO, and ABA treatments

To test the effect of chemicals on floral abscission, drugs were mixed with lanolin wax (Sigma) melted at 50°C and applied using sterile wooden toothpicks to the primary inflorescence of plants 35 days after germination. All chemicals were diluted from 100 mM stock solutions in dimethyl sulfoxide (Sigma) to the working concentrations of 50 μM for ABA (Duchefa), 500 μM for peroxynitrite ($ONOO^-$, Calbiochem), or 500 μM for the NO scavenger 2-(4-carboxyphenyl)-4,4,5,5-tetramethylimidazoline-l-oxyl3-oxide (cPTIO, Sigma).

Microscopy and histology

For toluidine blue (TB, Sigma, cat. n. 92-31-9) staining, flowers were dipped in 0.025% (w/v) TB solution in water for 2–3 min and washed with distilled water for 2 min. For β-glucuronidase (GUS) staining, flowers were incubated in GUS solution (3 mM potassium ferrocyanide, 3 mM potassium ferricyanide, 1 mM X-Gluc, 1 M NaH_2PO_4, 1 M Na_2HPO_4, 0.5 M EDTA, pH 8.0) for 6 h at 37°C and then rinsed in 70% (v/v) ethanol for at least 5 min. After removing chlorophyll in clearing solution (6:1 ethanol:acetic acid, v/v) several times, samples were rinsed using 70% (v/v) ethanol. To visualise superoxide accumulation in AZs, inflorescences were stained with nitroblue tetrazolium (NBT, TCI) (Wang *et al.*, 2017). The inflorescences were vacuum-infiltrated with NBT solution (0.05% [w/v] in phosphate buffered saline [PBS]) and incubated in the dark for 30 min. After staining, inflorescences were fixed and destained in 3:1:1 ethanol:lactic acid:glycerol (bleaching solution, v/v/v) at 70°C until chlorophyll was completely removed.

Low-magnification images were collected using a Leica stereomicroscope (M205FA, Leica). Confocal laser-scanning microscopy images were obtained using a Zeiss LSM 700 (with Zen SP3 Black edition). To determine subcellular localizations, flowers were incubated in half-strength Murashige and Skoog (MS) medium (2.2 g/L MS salt, 1% [w/v] sucrose, pH 5.7) with 0.1% (w/v) calcofluor white (Sigma-Aldrich, cat. n. 18909) and FM1-43 (Invitrogen, cat. n. F35355) for 30 min and then rinsed for 30 min with MS medium. The excitation and

emission windows were as follows: GFP (FM1-43), 488 nm and 500–530 nm; mCherry, 561 nm and 600–630 nm; and Calcofluor white, 405 nm and 425–475 nm.

Measurements of ABA contents

Approximately 100 mg of frozen stage 13 (S13) and S15 AZ samples was homogenised with two steel beads in a TissueLyser II (Qiagen) for 1 min at 26 Hz. Phytohormones were extracted as previously described (Joo *et al.*, 2021) with minor modifications. The samples were evaporated to near dryness in a centrifugal vacuum concentrator (VC2124, Gyrogen) at 30°C. The dried samples were dissolved in 500 mL 70% (v/v) methanol:water for analysis by high-performance liquid chromatography coupled to a triple-quadrupole mass spectrometer (LC-MS-8050, Shimadzu) as described previously (Joo *et al.*, 2021). The phytohormones were detected in negative electrospray ionization mode, and the detailed detection method followed that described by (Schäfer *et al.*, 2016). The amounts of phytohormones were normalised to the exact fresh mass of plant materials and internal standards for each phytohormone.

RNA extraction, cDNA synthesis, and reverse-transcription quantitative PCR (RT-qPCR)

AZ samples were collected by hand-cutting AZ regions from approximately 50 flowers of the wild type and the *msd2-1* mutant. Flowers suitable for the stage were collected only from the primary inflorescence. Total RNA was extracted from the AZ samples using an RNeasy Plant Mini kit (Qiagen) according to the manufacturer's instructions. Total RNA concentration and quality were measured using an ND-2000 spectrophotometer (Thermo Scientific). The RNA OD 260/280 ratios were 1.9–2.1, and OD 260/230 ratios were 2.0–2.5. RNA quality was monitored by running all samples on a TapeStation RNA screentape (Agilent). Samples with RNA integrity number >8.0 were used for RNA sequencing library construction.

A first-strand synthesis kit (GenDepot) with oligo(dT) primers was used for cDNA synthesis from 2 μg of total RNA according to the manufacturer's instructions. The resulting cDNAs were used for qPCR with a Quant Studio 1 (Applied Biosystems) instrument using SYBR Green Real-time PCR Master Mix (Applied Biosystems). Primer sequences are listed in Table S1. Threshold cycle (Ct) values were used to calculate $2^{-\Delta\Delta Ct}$ for expression analysis,

where ΔΔCt for treated plants was determined as follows: (Ct target gene – Ct *ACTIN* gene) – control plant (Ct target gene – Ct *ACTIN* gene) (Livak & Schmittgen, 2001).

Transcriptome deep sequencing (RNA-seq) library preparation and sequencing

RNA-seq libraries were independently prepared from 1 μg of total RNA for each sample using the TruSeq RNA Sample Prep Kit v2 (Illumina) according to the manufacturer's manual. Library quality and titre were verified using KAPA Library Quantification kits for Illumina Sequencing platforms according to the qPCR Quantification Protocol Guide (KAPA BIOSYSTEMS). Sequencing was performed on an Illumina NovaSeq instrument (Illumina, Inc), generating 100-bp paired-end reads. Library preparation and sequencing were performed by Macrogen (South Korea).

RNA-seq analysis and functional annotation

Reads for each sample were mapped to the reference genome (TAIR 10) and counted using RSEM 1.3.0 software and trimmed mean of M value–normalised transcripts per million (TPM) values were determined for each transcript (Li & Dewey, 2011). Differentially expressed genes (DEGs) were identified using EdgeR version 3.16.5 to calculate the negative binomial dispersion across conditions (Robinson *et al.*, 2010). Genes were determined to be differentially expressed if they showed a minimum two-fold change in expression, with a false discovery rate (FDR)–adjusted *P* value of <0.05. Functional annotation of DEGs was performed using Gene Ontology (GO) and Kyoto Encyclopedia of Genes and Genomes (KEGG) pathway enrichment analyses using DAVID (v6.8) (Huang *et al.*, 2009), and Web Gene Ontology Annotation Plot (WEGO) analysis using WEGO 2.0 (Ye *et al.*, 2018).

Statistical analysis

All statistical analyses were done with the SPSS statistical software package (v26, IBM). One-way analysis of variance (ANOVA) with post-hoc Tukey or Kruskal-Wallis with Dunn's multiple comparisons test was performed. Each experiment was repeated three times.

Results

Floral organ abscission is accelerated in *msd2* mutants

The timing of floral organ abscission is determined through the complex integration of various environmental changes and developmental signals (Sawicki *et al.*, 2015). ROS are important mediators of various environmental stress-related signalling pathways (Huang *et al.*, 2019) and might contribute to organ abscission, as they also accumulate in AZs (Sakamoto *et al.*, 2008a; Bar-Dror *et al.*, 2011; Yang *et al.*, 2015; Liao *et al.*, 2016; Lee *et al.*, 2018). To investigate the link between ROS and the timing of abscission, we focused on the secretory Mn SOD MSD2 (Chen *et al.*, 2022) and tested its role in regulating abscission. *MSD2* was preferentially expressed in the floral AZ starting in stage 13 (S13) flowers, when the buds open (Smyth *et al.*, 1990); *MSD2* expression levels increased as flower development progressed (Fig. **1a** and Fig. **S1a**). At S16, when floral organs wither and begin to fall, *MSD2* expression decreased in the AZ and showed a strong signal in the nectary, as determined with *MSD2pro:GUS* transgenic lines (Fig. **1a**). MSD2 harbours a secretory signal peptide in its N terminus and localises in the secretory pathways, including the vacuole or apoplast in seedlings (Chen *et al.*, 2022). We determined the accumulation pattern of MSD2 in the AZ of transgenic plants that ubiquitously express *MSD2-mCherry* under the control of the *UBIQUITIN 10* (*UBQ10*) promoter. We mainly detected MSD2-mCherry in the vacuole of residual cells (RECs), which are AZ cells of the receptacle, and in the apoplast of secession cells (SECs), which are AZ cells of the separating organs (Lee *et al.*, 2018) (Fig. **1b**).

To investigate the effects of MSD2 on abscission, we analysed the abscission phenotype of two independent T-DNA insertional mutants (Fig. **S1b** and **c**) (Chen *et al.*, 2022). In the *msd2-1* and *msd2-2* mutants, floral organ abscission occurred when fruit length was markedly shorter than that of the wild type (Fig. **1c**), suggesting that abscission starts earlier in *msd2* mutants. We obtained similar results when we analysed the embryonic developmental stage at the beginning of abscission. In the wild type, abscission took place mainly at the 2/4-cell stage of the embryo, whereas abscission occurred at a younger stage of embryonic development in *msd2* mutants, with the proportion of 1-cell stage embryos being higher in the S16 siliques of the *msd2-1* mutant compared to the wild type (Fig. **S1d**). Neither the number of siliques per inflorescence (Fig. **S1e** and **f**) nor the germination rates of seeds (Fig. **S1g** and **h**) were significantly different between the wild type and *msd2* mutants. Since abscission is closely related to flower development, abscission can be accelerated by promoting seed

development or by promoting the onset of abscission. The above results suggest that MSD2 has a direct effect on the onset of abscission without significantly affecting embryo development.

To quantify the phenotypes of *msd2* mutants, we measured silique length and the position of the first flowers at S16, when the floral organs begin to wither and fall (Fig. **1d** and **e**). Using both quantification methods, we confirmed the accelerated abscission in *msd2-1* and *msd2-2* mutant plants; this phenotype was rescued to that of the wild type upon overexpression of *MSD2* under the control of the *UBQ10* promoter in the *msd2-1* mutant background (Fig. **1c–e**). The phenotype of *msd2-2* was slightly weaker than that of *msd2-1* (Fig. **1e**), which could be attributed to the low level of RNA remaining *msd2-2* (Fig. **S1c**). During abscission, the AZ becomes permeable as the cell wall is hydrolysed, which can be visualised by staining with a hydrophilic dye such as toluidine blue (TB) (Tanaka *et al.*, 2004). In agreement with the results above, we confirmed the acceleration of abscission in *msd2* mutants by TB staining (Fig. **1f**).

To explore the possible correlation between the onset of abscission and ROS accumulation, we investigated the pattern of ROS accumulation by staining with nitroblue tetrazolium (NBT), which is highly sensitive to superoxide (Straus *et al.*, 2010). We observed earlier NBT staining of the AZ in *msd2-1* and *msd2-2* mutant plants compared to the wild type; again, this phenotype was restored to that seen in the wild type in the *msd2-1 UBQ10pro:MSD2* transgenic lines (Fig. **1g**). These results suggest that MSD2, which is involved in ROS metabolism, negatively regulates the timing of abscission.

MSD2 regulates the expression of *IDA* and *HAE* in the AZ

The IDA-HAE signalling pathway plays an important role in regulating the expression of cell wall-modifying enzymes responsible for cell wall hydrolysis during abscission (Cho *et al.*, 2008; Stenvik *et al.*, 2008; Aalen *et al.*, 2013; Patharkar & Walker, 2015). To investigate the possible relationship between MSD2 and the IDA-HAE pathway for the regulation of abscission onset, we determined the expression of *IDA* and *HAE* in the *msd2-1* mutant with the *GUS* reporter gene driven by the *IDA* or *HAE* promoters. The expression of *IDA* and *HAE* increased during S15–16, when abscission is activated and floral organs begin to shed (Butenko *et al.*, 2003; Cai & Lashbrook, 2008; Leslie *et al.*, 2010; Patharkar & Walker, 2015). We observed a similar expression pattern with our *IDApro:GUS* and *HAEpro:GUS* reporter lines,

which was altered in *msd2-1* mutants (Fig. **2a**). In the *msd2-1* mutant, the spatial expression patterns of *IDA* and *HAE* were similar to those in the wild type, but the temporal patterns were altered. We detected GUS staining in an earlier position compared to the wild type for both *IDA* and *HAE* reporters, which was consistent with the early onset of abscission in the *msd2-1* mutant (Fig. **1c–e**). We confirmed the acceleration of the temporal expression pattern of *IDA* and *HAE* through RT-qPCR analysis by position, and observed a similar earlier shift in the expression of *HSL2* (Fig. **2b**). Unlike the change in the timing of their expression, the expression levels of these genes did not differ significantly between the wild type and the *msd2-1* mutant (Fig. **S2**), suggesting that the temporal difference rather than the quantitative difference in *IDA* and *HAE* transcript levels is the major change associated with the *msd2-1* mutant. The accelerated abscission caused by the loss of MSD2 function was abolished when the *msd2-1* mutation was introduced into the *hae hsl2* double mutant background. Indeed, the *hae hsl2 msd2-1* triple mutant exhibited abscission phenotypes similar to the *hae hsl2* double mutant (Fig. **2c**). These results suggest that MSD2 acts upstream of the IDA-HAE pathway, regulating the expression of the encoding genes and thus influencing the timing of abscission.

Genome-wide transcriptome analysis

To explore the pathways regulating the expression of *IDA* and *HAE* in the *msd2-1* mutant, we conducted a comparative transcriptome analysis between the wild type and the *msd2-1* mutant by RNA-seq. To this end, we collected AZ samples by hand-cutting AZ regions from approximately 50 flowers at S13 and S15 from the wild type and the *msd2-1* mutant. The progression of flower development from S13 to S15 was accompanied by changes in the expression of many genes in both genotypes, with 3,966 differentially expressed genes (DEGs) in the wild type and 3,511 DEGs in the *msd2-1* mutant (Fig. **3a** and **b**). When comparing the wild type and mutant, we identified 875 DEGs at S13 (406 genes upregulated and 469 genes downregulated in the *msd2-1* mutant) and 295 DEGs at S15 (185 genes upregulated and 110 genes downregulated in the *msd2-1* mutant) (Fig. **3b** and **c,** Table **S2**). To understand the biological functions of these DEGs in the *msd2-1* mutant, we performed a GO enrichment analysis, using the DEGs at each stage. This analysis revealed terms related to phytohormone responses including ABA, auxin, and JA, and responses to a wide range of stress stimuli, including nitrate, oxidative stress, cold, and pathogens (Fig. **3d**, Table **S3-5**). KEGG pathway analysis also indicated that the expression of genes involved in nitric oxide (NO) compound

biosynthetic processes is affected in the *msd2-1* mutant (Fig. **S3** and Table **S6**).

The timing of abscission is determined by integrating environmental changes along with a programmed developmental process. Therefore, we hypothesised that ABA and NO, which are important signalling molecules responding to environmental stress (Mur *et al.*, 2013; Ma *et al.*, 2018), may also play a role in MSD2-related abscission. The total number of DEGs between the wild type and the *msd2-1* mutant was lower at S15 compared to S13, but we identified more DEGs associated with NO and ABA responses at S15 (Fig. **3c–f**). Among the NO- and ABA-responsive genes with altered expression levels at S15 flowers of the *msd2-1* mutant compared to the wild type, many showed stage-dependent expression changes in the wild type (Fig. **3e** and **f**). Therefore, the expression of these genes in the wild type were closely linked with abscission development, and their expression patterns were further enhanced in the *msd2-1* mutant. This result suggested that NO and ABA responses are part of the intrinsic abscission process and that these responses are enhanced in the *msd2-1* mutant. In contrast to the ABA-responsive genes that showed higher expression levels at S15 in the *msd2-1* mutant compared to the wild type, the expression pattern of genes involved in ABA biosynthesis or recognition of ABA signalling were not significantly different between the wild type and the mutant. In addition, genes encoding negative regulators of ABA signalling were strongly upregulated in the *msd2-1* mutant compared to the wild type at S15 (Fig. **3g** and Fig. **S4**). We validated these observations by RT-qPCR (Fig. **S5**). These results suggest that MSD2 affects abscission by modulating ABA signalling rather than via ABA biosynthetic pathways, and that the process is accompanied by a feedback loop that upregulates the expression of negative regulators such as protein phosphatase 2Cs (PP2Cs).

Accelerated abscission in the *msd2-1* mutant is mediated by NO

RNA-seq analysis suggested that NO may contribute to regulating abscission and that MSD2 may negatively regulate NO-mediated signalling. To determine whether NO plays a role in abscission, we visualised NO accumulation in the AZ by 4,5-diaminofluorescein diacetate (DAF-2DA) staining (He *et al.*, 2004; Planchet & Kaiser, 2006; Vishwakarma *et al.*, 2019; Duan *et al.*, 2020). Fluorescence measurement is possible only after the floral organs are removed. To avoid damage and induction of wounding signalling, we performed this experiment on S16 flowers, when floral organs naturally detach. We detected DAF-2DA

fluorescence in S16 AZs that decreased upon treatment with the NO scavenger 2-(4-carboxyphenyl)-4,4,5,5-tetramethylimidazoline-l-oxyl3-oxide (cPTIO) (Planchet & Kaiser, 2006; Vishwakarma *et al.*, 2019; Duan *et al.*, 2020), demonstrating the specificity of the signal (Fig. **4a**). The *msd2-1* mutant exhibited higher fluorescence intensity than the wild type (Fig. **4a** and **b**), suggesting higher NO accumulation in the *msd2-1* mutant.

To investigate whether NO induces abscission, we applied lanolin wax containing 500 μM peroxynitrite ($ONOO^-$) to inflorescence stems and recorded the state of floral organ abscission 5 days later. Peroxynitrite treatment dramatically accelerated abscission, whereas cPTIO treatment delayed abscission (Fig. **4c–e**). Simultaneous treatment of inflorescences with peroxynitrite and cPTIO blocked the abscission-promoting effects of peroxynitrite (Fig. **4c–e**). Similarly, treating the *msd2-1* mutant with cPTIO also suppressed the abscission-promoting effects associated with the loss of MSD2 (Fig. **4f–h**). These results suggest that accelerated abscission in *msd2* mutants is mediated by NO.

Interaction of ABA with NO is important for regulating abscission

The RNA-seq analysis above also suggested ABA signalling as another downstream target for the MSD2-mediated regulation of abscission. To test the role of ABA in floral organ abscission in Arabidopsis, we measured ABA contents in the AZ: ABA levels increased with developmental stage in both wild-type and *msd2-1* flowers (Fig. **5a**). To directly observe the effects of ABA on floral abscission, we applied lanolin wax containing ABA to inflorescence stems and scored floral abscission 5 days after treatment. We observed a dramatic promotion of abscission by ABA (Fig. **5b–d**). Abscission was delayed in the *abi5-7* mutant (*ABA insensitive 5*), providing an important control for the specificity of the response (Fig. **5e–g**).

To elucidate the interaction between ABA and NO during abscission, we tested the effect of simultaneous treatment with ABA and the NO scavenger. Co-treatment of inflorescences with cPTIO and ABA suppressed the promotion of abscission mediated by ABA (Fig. **5b–d**). In addition, the expression levels of *ABI5* and the ABA-responsive genes *ABI1* and *ABRE BINDING FACTOR4* (*ABF4*) rose in response to exogenously supplied peroxynitrite (Fig. **5h**). Just as the expression of ABA-responsive genes was regulated by NO, we determined that the expression of NO-responsive genes is also regulated by ABA. Expression of the NO-responsive genes *GLUTATHIONE S-TRANSFERASE6* (*GSTF6*) and *LIPOXYGENASE 4*

(*LOX4*) (Ahlfors *et al.*, 2009; Gaudinier *et al.*, 2018) was upregulated by ABA treatment as well as peroxynitrite treatment (Fig. **5h**). These results suggest that ABA and NO interact to determine the timing of abscission.

NO and ABA affect abscission by regulating the expression of *IDA* and *HAE*

To determine the relationship between NO, ABA, and the IDA-HAE module, we tested the effects of NO and ABA on abscission in *ida* and *hae hsl2* mutants. We observed that abscission is slightly accelerated by NO and ABA treatment in *ida* mutants (Fig. **6a-c**), while similar treatments had no effect in the *hae hsl2* double mutant (Fig. **6d**). However, the expression of ABA- and NO-responsive genes increased in S15 flowers of both the *ida* and *hae hsl2* mutants after NO and ABA treatment (Fig. **6e**), suggesting that NO and ABA act upstream of the IDA-HAE module. To assess whether the expression of *IDA* and *HAE* is modulated by NO and ABA, we dissected the spatiotemporal expression patterns of *IDA* and *HAE* using our *GUS* reporter lines. Treatment with peroxynitrite or ABA did not affect the spatial expression pattern of these genes but did affect their temporal expression pattern; we detected GUS signals earlier under these treatments than under the control condition (Fig. **6f** and **g**). We confirmed these results by RT-qPCR for *IDA* and *HAE* transcript levels under control and treated conditions in S15 flowers (Fig. **6h**). Taken together, our data suggest that alterations in ROS metabolism in the *msd2-1* mutant promote the accumulation of NO and activate ABA signalling, which in turn induces abscission by regulating the expression timing of *IDA* and *HAE*.

Discussion

Floral organ abscission is directly affected by flower development and fertilisation but also reacts to changes in the outside environment (Addicott, 1982; Taylor & Whitelaw, 2001). Although a multi-layered regulatory mechanism to initiate abscission is likely to be required to comprehensively integrate these various external factors, our understanding of the entire signalling cascade is still fragmentary. In this study, we propose that ROS metabolism regulated by MSD2 contributes to one of the regulatory layers of abscission. While the regulation of ROS-generating enzymes has been intensively studied, the metabolism of the ROS they generate and the pathways activated by ROS remain largely unknown in the context of abscission, largely because the extracellular SOD had not been identified in Arabidopsis. None

of the seven classic SODs reported in Arabidopsis have a secretory signal peptide (Kliebenstein *et al.*, 1998). In this study, we show that *MSD2*, recently shown to encode a secretory Mn SOD (Chen *et al.*, 2022), is preferentially expressed in the AZ and is involved in the regulation of ROS metabolism. ROS levels regulated by MSD2 appeared to play an essential role in the correct timing of abscission, with both NO and ABA signals contributing to this effect, to regulate the expression of *IDA* and *HAE* as the downstream targets of ROS and MSD2. Our findings suggest another layer that regulates ROS signalling, which helps to understand the complexity of the integration of external signals into endogenous developmental programs.

The name ABA was coined in light of the discovery that the phytohormone induced abscission in young cotton (*Gossypium hirsutum*) fruit (Ohkuma *et al.*, 1963; Cornforth *et al.*, 1965; Addicott *et al.*, 1968). However, it was later suggested that the observed abscission was an indirect effect of elevated ethylene levels (Cracker & Abeles, 1969), and the roles of ABA in abscission have not received much attention since. Indirect roles of ABA on floral abscission were recently demonstrated in Arabidopsis as well (Ogawa *et al.*, 2009). The ABA-deficient mutant *aba2-2* exhibits normal floral organ abscission, while the *ein2-1 aba2-2* double mutant shows an abscission phenotype similar to that of the *ein2-1* (*ethylene insensitive 2-1*) single mutant. However, a triple mutant between *ein2-1*, *aba2-2*, and *aos* (defective in ALLENE OXIDE SYNTHASE, involved in JA biosynthesis) displayed a very severe abscission delay relative to the wild type and the *ein2-1* mutant, suggesting partially redundant roles for the three phytohormones ethylene, ABA, and JA in abscission. Stage-specific transcriptome analysis also confirmed the interplay between the three phytohormones (Niederhuth *et al.*, 2013). The expression of ethylene and ABA signalling and biosynthesis-related genes increases at S15, while the expression of JA signalling-related genes decreases, in both the wild type and the *hae hsl2* double mutant, suggesting that phytohormone regulation is independent of HAE.

In contrast to previous studies in which abscission was normal in the ABA-deficient mutant *aba2-2* (Niederhuth *et al.*, 2013), we observed a delay in floral organ abscission in the *abi5-7* mutant (Fig. **5**). These results suggest the possibility that ABI5 may regulate abscission separately from its role in ABA signalling. ABI5 is a basic leucine zipper transcription factor whose activity is regulated via protein–protein interactions and posttranslational modifications. Although ABI5 is a well-known master regulator of ABA signalling, *ABI5* expression and ABI5 activity and stability are regulated by various phytohormones, and ABI5 serves as an integration hub (Skubacz *et al.*, 2016; Collin *et al.*, 2021). Evaluating how the activity of ABI5

is regulated in the AZ will be important for understanding the effects of ABA on abscission and crosstalk with other phytohormones. Furthermore, we observed no significant changes for the expression of ABA biosynthesis–related genes such as *ABA3*, *NINE-CIS-EPOXYCAROTENOID DIOXYGENASE5* (*NCED5*), or *NCED6* (Fig. **3**) or for ABA contents (Fig. **5**) in the *msd2-1* mutant. Since these changes were not quantified over time, we cannot exclude that the timing of ABA biosynthesis in the *msd2-1* mutant may have accelerated as well. However, it is also possible that the increased expression levels of ABA-responsive genes in the *msd2-1* mutant are the result of direct control of ABA signalling rather than ABA biosynthesis. The protein phosphatase 2Cs ABI1 and ABI2 are negative regulators of ABA signalling and are redox-sensitive, as their activity can be inactivated by ROS (Meinhard & Grill, 2001; Meinhard *et al.*, 2002; Sierla *et al.*, 2016). Mitogen-activated protein kinases activated by the ABA core signalling pathway (de Zelicourt *et al.*, 2016) are also downstream targets of ROS (Lee *et al.*, 2016). Among the various possibilities of activating ABA signalling by ROS, elucidating which pathways are actually regulated in *msd2* mutants remains a major challenge.

There is growing evidence that NO acts as a plant physiological mediator in various developmental and stress responses (Domingos *et al.*, 2015; Farnese *et al.*, 2016). NO affects senescence and abscission of the rudimentary leaves in lychee (*Litchi chinensis*) (Yang *et al.*, 2018). ROS might participate in the signalling cascade leading to NO biosynthesis (Gaupels *et al.*, 2011; Farnese *et al.*, 2016), but the understanding of this process is very limited, mainly because NO biosynthesis is not yet fully understood. Nitrate reductase (NR), a cytosolic enzyme essential for nitrogen assimilation, has been proposed to be involved in NO production in a variety of physiological processes (Hao *et al.*, 2010; Mur *et al.*, 2013; Chamizo-Ampudia *et al.*, 2017). However, important issues remain unresolved. Under normal growth conditions, NR preferentially reduces nitrate (NO_3^-) to nitrite (NO_2^-) because NR prefers nitrate over nitrite. Currently, NR appears to require specific conditions, such as anaerobic conditions or high nitrite concentrations, to produce any significant amounts of NO (Mur *et al.*, 2013; Farnese *et al.*, 2016). NO synthase (NOS), the main enzymatic source for NO in animals, has also been widely considered as another candidate for NO biosynthesis. Several reports acknowledge the possible existence of NOS activity in plants (Corpas *et al.*, 2009; Astier *et al.*, 2018), but the associated protein has yet to be identified (Jeandroz *et al.*, 2016; Santolini *et al.*, 2017). Future exploration into the interactions between ROS, NO, and ABA that take place during abscission may uncover as-yet-unknown upstream regulatory pathways of NO

biosynthesis or novel NO-related messengers.

The onset of floral organ abscission is determined by integrating fertilisation, the age of floral organs, and environmental conditions, at the centre of which the interaction between the plant phytohormones ethylene, ABA, and JA plays a fundamental role (Ogawa *et al.*, 2009; Estornell *et al.*, 2013; Sawicki *et al.*, 2015). In particular, ethylene plays central roles in determining the onset of floral organ abscission in Arabidopsis (Meir *et al.*, 2019). Floral organ abscission does occur in the ethylene-insensitive mutants *etr1-1* (*ethylene triple response 1-1*) and *ein2-1*, though with a dramatic delay relative to the wild type (Patterson & Bleecker, 2004). While the interplay between phytohormones is important to determine the onset of abscission, IDA-HAE may play a key role in the execution of organ shedding (Roberts & Gonzalez-Carranza, 2007; Cho *et al.*, 2008). The signalling cascades and transcription factor networks downstream of IDA-HAE are well described (Cho *et al.*, 2008; Patharkar & Walker, 2015), but the regulatory mechanisms upstream of IDA-HAE are relatively poorly understood. The expression of *IDA* and *IDA-LIKE* (*IDL*) is dependent on ethylene signalling (Butenko *et al.*, 2006) and responds to abiotic and biotic stress conditions (Vie *et al.*, 2015), suggesting that the IDA-HAE module plays a role in linking stress responses to development. The elucidation of additional regulatory circuits regulating the expression of *IDA* and *HAE* is necessary to reflect the underlying complexity associated with the integration of multiple signals.

In this study, we propose that ROS metabolism, which is regulated by MSD2 and affects NO and ABA signalling components, is a novel upstream module that regulates the expression of *IDA* and *HAE*. Further elucidation of how the activity of MSD2 or the expression of *MSD2* is regulated under various environmental conditions is necessary for a comprehensive understanding of the biological significance of ROS metabolism regulated by MSD2. ROS and IDA-HAE are involved in cell separation and responses to stress in various cell types, the mechanisms of which are conserved in various plants (Tucker & Yang, 2012; Ventimilla *et al.*, 2020; Ventimilla *et al.*, 2021), suggesting that our findings should be applicable to other cell types and other plant species, including crops. Protein concentration is often controlled not only through synthesis but also through the balance of synthesis and degradation (Vierstra, 1993), which has the advantage of being able to respond quickly to needs. Our findings suggest that ROS concentrations are similarly regulated through a balance between production and degradation, which is thought to be broadly applicable to various signal transduction processes beyond abscission.

Acknowledgements

We thank Niko Geldner (UNIL) for critical reading of the manuscript and H. Ryu (Chungbuk National University) for sharing *abi5-7* mutant seeds. Y.L. was funded by the Suh Kyungbae Foundation (SUHF-19010003) and the National Research Foundation of Korea (NRF-2020R1A2C2013176 and NRF-2021R1A5A1032428). J.L. was funded by the National Research Foundation of Korea (NRF-2020R1I1A1A01068615). H.C. was supported by the China Scholarship Council (CSC202008140062) and the Natural Science Foundation of China (NSFC31900251).

Author contributions

Y.L. and J.L. conceived the study and designed the experiments. J.L., H.C., G.L., A.E., and S.-G.K. performed the experiments. D.S. and J.L. analysed the RNA-seq data. Y.L. and J.L. wrote the manuscript. All authors have read and agreed to the published version of the manuscript.

Data availability

The raw data files for the RNA-seq analysis reported in this paper can be found at GenBank under the accession number PRJNA786431.

Competing interests

None declared.

References

Aalen RB, Wildhagen M, Sto IM, Butenko MA. 2013. IDA: a peptide ligand regulating cell s eparation processes in Arabidopsis. *J Exp Bot* **64**(17): 5253-5261.

Addicott FT. 1982. *Abscission*. Berkeley: University of California Press.

Addicott FT, Lyon JL, Ohkuma K, Thiessen WE, Carns HR, Smith OE, Cornforth JW, Milborrow BV, Ryback G, Wareing PF. 1968. Abscisic acid: a new name for abscisin II (dormin). *Science* **159**(3822): 1493.

Ahlfors R, Brosché M, Kollist H, Kangasjärvi J. 2009. Nitric oxide modulates ozone-induced cell death, hormone biosynthesis and gene expression in Arabidopsis thaliana. *The Plant Journal* **58**(1): 1-12.

Astier J, Gross I, Durner J. 2018. Nitric oxide production in plants: an update. *J Exp Bot* **69**(14): 3401-3411.

Bar-Dror T, Dermastia M, Kladnik A, Znidaric MT, Novak MP, Meir S, Burd S, Philosoph-Hadas S, Ori N, Sonego L, et al. 2011. Programmed cell death occurs asymmetrically during abscission in tomato. *Plant Cell* **23**(11): 4146-4163.

Butenko MA, Patterson SE, Grini PE, Stenvik GE, Amundsen SS, Mandal A, Aalen RB. 2003. Inflorescence deficient in abscission controls floral organ abscission in Arabidopsis and identifies a novel family of putative ligands in plants. *Plant Cell* **15**(10): 2296-2307.

Butenko MA, Stenvik GE, Alm V, Saether B, Patterson SE, Aalen RB. 2006. Ethylene-dependent and -independent pathways controlling floral abscission are revealed to converge using promoter :: reporter gene constructs in the ida abscission mutant. *Journal of Experimental Botany* **57**(14): 3627-3637.

Cai S, Lashbrook CC. 2008. Stamen abscission zone transcriptome profiling reveals new candidates for abscission control: enhanced retention of floral organs in transgenic plants overexpressing Arabidopsis ZINC FINGER PROTEIN2. *Plant Physiology* **146**(3): 1305-1321.

Chamizo-Ampudia A, Sanz-Luque E, Llamas A, Galvan A, Fernandez E. 2017. Nitrate Reductase Regulates Plant Nitric Oxide Homeostasis. *Trends Plant Sci* **22**(2): 163-174.

Chen H, Lee J, Lee JM, Han M, Emonet A, Lee J, Jia X, Lee Y. 2022. MSD2, an apoplastic Mn-SOD, contributes to root skotomorphogenic growth by modulating ROS distribution in Arabidopsis. *Plant Science* **317**: 111192.

Cho SK, Larue CT, Chevalier D, Wang H, Jinn TL, Zhang S, Walker JC. 2008. Regulation of floral organ abscission in Arabidopsis thaliana. *Proc Natl Acad Sci U S A* **105**(40): 15629-15634.

Collin A, Daszkowska-Golec A, Szarejko I. 2021. Updates on the Role of ABSCISIC ACID INSENSITIVE 5 (ABI5) and ABSCISIC ACID-RESPONSIVE ELEMENT BINDING FACTORs (ABFs) in ABA Signaling in Different Developmental Stages in Plants. *Cells* **10**(8): 1996.

Cornforth JW, Milborrow BV, Ryback G. 1965. Chemistry and Physiology of Dormins in Sycamore. *Nature* **205**(4978): 1269-1270.

Corpas FJ, Palma JM, Del Rio LA, Barroso JB. 2009. Evidence supporting the existence of L-arginine-dependent nitric oxide synthase activity in plants. *New Phytol* **184**(1): 9-14.

Cracker LE, Abeles FB. 1969. Abscission: role of abscisic Acid. *Plant Physiol* **44**(8): 1144-1149.

de Zelicourt A, Colcombet J, Hirt H. 2016. The Role of MAPK Modules and ABA during Abiotic Stress Signaling. *Trends Plant Sci* **21**(8): 677-685.

Domingos P, Prado AM, Wong A, Gehring C, Feijo JA. 2015. Nitric oxide: a multitasked signaling gas in plants. *Mol Plant* **8**(4): 506-520.

Duan Q, Liu MJ, Kita D, Jordan SS, Yeh FJ, Yvon R, Carpenter H, Federico AN, Garcia-Valencia LE, Eyles SJ, et al. 2020. FERONIA controls pectin- and nitric oxide-mediated male-female interaction. *Nature* **579**(7800): 561-566.

Dunand C, Crèvecoeur M, Penel C. 2007. Distribution of superoxide and hydrogen peroxide in Arabidopsis root and their influence on root development: possible interaction with peroxidases. *New Phytologist* **174**(2): 332-341.

Dvorak P, Krasylenko Y, Ovecka M, Basheer J, Zapletalova V, Samaj J, Takac T. 2021. In vivo light-sheet microscopy resolves localisation patterns of FSD1, a superoxide dismutase with function in root development and osmoprotection. *Plant Cell Environ* **44**(1): 68-87.

Dvorak P, Krasylenko Y, Zeiner A, Samaj J, Takac T. 2020. Signaling Toward Reactive Oxygen Species-Scavenging Enzymes in Plants. *Front Plant Sci* **11**: 618835.

Estornell LH, Agustí J, Merelo P, Talón M, Tadeo FR. 2013. Elucidating mechanisms underlying organ abscission. *Plant Science* **199**: 48-60.

Farnese FS, Menezes-Silva PE, Gusman GS, Oliveira JA. 2016. When Bad Guys Become Good Ones: The Key Role of Reactive Oxygen Species and Nitric Oxide in the Plant Responses to Abiotic Stress. *Front Plant Sci* **7**: 471.

Gaudinier A, Rodriguez-Medina J, Zhang L, Olson A, Liseron-Monfils C, Bågman A-M, Foret J, Abbitt S, Tang M, Li B. 2018. Transcriptional regulation of nitrogen-associated metabolism and growth. *Nature* **563**(7730): 259-264.

Gaupels F, Kuruthukulangarakoola GT, Durner J. 2011. Upstream and downstream signals of nitric oxide in pathogen defence. *Current opinion in plant biology* **14**(6): 707-714.

Hao F, Zhao S, Dong H, Zhang H, Sun L, Miao C. 2010. Nia1 and Nia2 are involved in exogenous salicylic acid-induced nitric oxide generation and stomatal closure in Arabidopsis. *J Integr Plant Biol* **52**(3): 298-307.

He Y, Tang RH, Hao Y, Stevens RD, Cook CW, Ahn SM, Jing L, Yang Z, Chen L, Guo F, et al. 2004. Nitric oxide represses the Arabidopsis floral transition. *Science* **305**(5692): 1968-1971.

Hu SH, Lin SF, Huang YC, Huang CH, Kuo WY, Jinn TL. 2021. Significance of AtMTM1 and AtMTM2 for Mitochondrial MnSOD Activation in Arabidopsis. *Front Plant Sci* **12**: 690064.

Huang CH, Kuo WY, Weiss C, Jinn TL. 2012. Copper chaperone-dependent and -independent activation of three copper-zinc superoxide dismutase homologs localized in different cellular compartments in Arabidopsis. *Plant Physiol* **158**(2): 737-746.

Huang DW, Sherman BT, Lempicki RA. 2009. Systematic and integrative analysis of large gene lists using DAVID bioinformatics resources. *Nature protocols* **4**(1): 44-57.

Huang H, Ullah F, Zhou D-X, Yi M, Zhao Y. 2019. Mechanisms of ROS Regulation of Plant

Development and Stress Responses. *Frontiers in Plant Science* **10**: 800.

Jeandroz S, Wipf D, Stuehr DJ, Lamattina L, Melkonian M, Tian Z, Zhu Y, Carpenter EJ, Wong GK, Wendehenne D. 2016. Occurrence, structure, and evolution of nitric oxide synthase-like proteins in the plant kingdom. *Sci Signal* **9**(417): re2.

Joo Y, Kim H, Kang M, Lee G, Choung S, Kaur H, Oh S, Choi JW, Ralph J, Baldwin IT. 2021. Pith-specific lignification in Nicotiana attenuata as a defense against a stem-boring herbivore. *New Phytologist* **232:** 332-344.

Kim J, Dotson B, Rey C, Lindsey J, Bleecker AB, Binder BM, Patterson SE. 2013. New Cloth es for the Jasmonic Acid Receptor COI1: Delayed Abscission, Meristem Arrest and Apic al Dominance. *Plos One* **8**(4): e60505.

Kliebenstein DJ, Monde RA, Last RL. 1998. Superoxide dismutase in Arabidopsis: an eclectic enzyme family with disparate regulation and protein localization. *Plant Physiol* **118**(2): 637-650.

Kumpf RP, Shi C-L, Larrieu A, Stø IM, Butenko MA, Péret B, Riiser ES, Bennett MJ, Aalen RB. 2013. Floral organ abscission peptide IDA and its HAE/HSL2 receptors control cell separation during lateral root emergence. *Proceedings of the National Academy of Sciences* **110**(13): 5235-5240.

Lee Y, Kim YJ, Kim MH, Kwak JM. 2016. MAPK Cascades in Guard Cell Signal Transduction. *Front Plant Sci* **7**: 80.

Lee Y, Yoon TH, Lee J, Jeon SY, Lee JH, Lee MK, Chen H, Yun J, Oh SY, Wen X, et al. 2018. A Lignin Molecular Brace Controls Precision Processing of Cell Walls Critical for Surface Integrity in Arabidopsis. *Cell* **173**(6): 1468-1480 e1469.

Leslie ME, Lewis MW, Youn J-Y, Daniels MJ, Liljegren SJ. 2010. The EVERSHED receptor-like kinase modulates floral organ shedding in Arabidopsis. *Development* **137**(3): 467-476.

Li B, Dewey CN. 2011. RSEM: accurate transcript quantification from RNA-Seq data with or without a reference genome. *BMC bioinformatics* **12**(1): 1-16.

Liao W, Wang G, Li Y, Wang B, Zhang P, Peng M. 2016. Reactive oxygen species regulate leaf pulvinus abscission zone cell separation in response to water-deficit stress in cassava. *Sci Rep* **6**: 21542.

Liu B, Butenko MA, Shi CL, Bolivar JL, Winge P, Stenvik GE, Vie AK, Leslie ME, Brembu T, Kristiansen W, et al. 2013. NEVERSHED and INFLORESCENCE DEFICIENT IN ABSCISSION are differentially required for cell expansion and cell separation during floral organ abscission in Arabidopsis thaliana. *J Exp Bot* **64**(17): 5345-5357.

Livak KJ, Schmittgen TD. 2001. Analysis of relative gene expression data using real-time quantitative PCR and the $2^{-\Delta\Delta CT}$ method. *methods* **25**(4): 402-408.

Ma Y, Cao J, He J, Chen Q, Li X, Yang Y. 2018. Molecular mechanism for the regulation of ABA homeostasis during plant development and stress responses. *International journal of molecular sciences* **19**(11): 3643.

Mckim SM, Stenvik GE, Butenko MA, Kristiansen W, Cho SK, Hepworth SR, Aalen RB, Hau

ghn GW. 2008. The BLADE-ON-PETIOLE genes are essential for abscission zone format ion in Arabidopsis. *Development* **135**(8): 1537-1546.

Meinhard M, Grill E. 2001. Hydrogen peroxide is a regulator of ABI1, a protein phosphatase 2C from Arabidopsis. *Febs Letters* **508**(3): 443-446.

Meinhard M, Rodriguez PL, Grill E. 2002. The sensitivity of ABI2 to hydrogen peroxide links the abscisic acid-response regulator to redox signalling. *Planta* **214**(5): 775-782.

Meir S, Philosoph-Hadas S, Riov J, Tucker ML, Patterson SE, Roberts JA. 2019. Re-evaluatio n of the ethylene-dependent and -independent pathways in the regulation of floral an d organ abscission. *J Exp Bot* **70**(5): 1461-1467.

Meng X, Zhou J, Tang J, Li B, de Oliveira MV, Chai J, He P, Shan L. 2016. Ligand-induced receptor-like kinase complex regulates floral organ abscission in Arabidopsis. *Cell repor ts* **14**(6): 1330-1338.

Mhamdi A, Van Breusegem F. 2018. Reactive oxygen species in plant development. *Develop ment* **145**(15): dev164376.

Mittler R, Vanderauwera S, Suzuki N, Miller G, Tognetti VB, Vandepoele K, Gollery M, Shu laev V, Van Breusegem F. 2011. ROS signaling: the new wave? *Trends in plant scienc e* **16**(6): 300-309.

Morgan MJ, Lehmann M, Schwarzlander M, Baxter CJ, Sienkiewicz-Porzucek A, Williams T C, Schauer N, Fernie AR, Fricker MD, Ratcliffe RG, et al. 2008. Decrease in mangan ese superoxide dismutase leads to reduced root growth and affects tricarboxylic acid c ycle flux and mitochondrial redox homeostasis. *Plant Physiol* **147**(1): 101-114.

Muller K, Linkies A, Vreeburg RA, Fry SC, Krieger-Liszkay A, Leubner-Metzger G. 2009. In vivo cell wall loosening by hydroxyl radicals during cress seed germination and elonga tion growth. *Plant Physiology* **150**(4): 1855-1865.

Mur LA, Mandon J, Persijn S, Cristescu SM, Moshkov IE, Novikova GV, Hall MA, Harren FJ , Hebelstrup KH, Gupta KJ. 2013. Nitric oxide in plants: an assessment of the current state of knowledge. *AoB PLANTS* **5**: pls052.

Myouga F, Hosoda C, Umezawa T, Iizumi H, Kuromori T, Motohashi R, Shono Y, Nagata N , Ikeuchi M, Shinozaki K. 2008. A Heterocomplex of Iron Superoxide Dismutases Defe nds Chloroplast Nucleoids against Oxidative Stress and Is Essential for Chloroplast Dev elopment in Arabidopsis. *Plant Cell* **20**(11): 3148-3162.

Niederhuth CE, Patharkar OR, Walker JC. 2013. Transcriptional profiling of the Arabidopsis a bscission mutant hae hsl2 by RNA-Seq. *BMC Genomics* **14**: 37.

Ogawa M, Kay P, Wilson S, Swain SM. 2009. ARABIDOPSIS DEHISCENCE ZONE POLYGALACT URONASE1 (ADPG1), ADPG2, and QUARTET2 are Polygalacturonases required for cell s eparation during reproductive development in Arabidopsis. *Plant Cell* **21**(1): 216-233.

Ohkuma K, Lyon JL, Addicott FT, Smith OE. 1963. Abscisin II, an Abscission-Accelerating Sub stance from Young Cotton Fruit. *Science* **142**(3599): 1592-1593.

Patharkar OR, Walker JC. 2015. Floral organ abscission is regulated by a positive feedback lo

op. *Proc Natl Acad Sci U S A* **112**(9): 2906-2911.

Patharkar OR, Walker JC. 2019. Connections between abscission, dehiscence, pathogen defen se, drought tolerance, and senescence. *Plant Science* **284**: 25-29.

Patterson SE, Bleecker AB. 2004. Ethylene-dependent and -independent processes associated with floral organ abscission in Arabidopsis. *Plant Physiol* **134**(1): 194-203.

Planchet E, Kaiser WM. 2006. Nitric oxide (NO) detection by DAF fluorescence and chemilum inescence: a comparison using abiotic and biotic NO sources. *Journal of Experimental Botany* **57**(12): 3043-3055.

Qi J, Wang J, Gong Z, Zhou JM. 2017. Apoplastic ROS signaling in plant immunity. *Curr Opi n Plant Biol* **38**: 92-100.

Roberts JA, Gonzalez-Carranza Z. 2007. *Plant cell separation and adhesion*: Oxford, UK: Black well.

Robinson MD, McCarthy DJ, Smyth GK. 2010. edgeR: a Bioconductor package for differential expression analysis of digital gene expression data. *Bioinformatics* **26**(1): 139-140.

Sakamoto M, Munemura I, Tomita R, Kobayashi K. 2008a. Involvement of hydrogen peroxid e in leaf abscission signaling, revealed by analysis with an in vitro abscission system in Capsicum plants. *Plant J* **56**(1): 13-27.

Sakamoto M, Munemura I, Tomita R, Kobayashi K. 2008b. Reactive oxygen species in leaf a bscission signaling. *Plant Signal Behav* **3**(11): 1014-1015.

Santolini J, Andre F, Jeandroz S, Wendehenne D. 2017. Nitric oxide synthase in plants: Whe re do we stand? *Nitric Oxide* **63**: 30-38.

Sawicki M, Aït Barka E, Clément C, Vaillant-Gaveau N, Jacquard C. 2015. Cross-talk betwee n environmental stresses and plant metabolism during reproductive organ abscission. *J ournal of Experimental Botany* **66**(7): 1707-1719.

Schäfer M, Brütting C, Baldwin IT, Kallenbach M. 2016. High-throughput quantification of m ore than 100 primary-and secondary-metabolites, and phytohormones by a single solid -phase extraction based sample preparation with analysis by UHPLC–HESI–MS/MS. *Plan t Methods* **12**(1): 1-18.

Shi C-L, Von Wangenheim D, Herrmann U, Wildhagen M, Kulik I, Kopf A, Ishida T, Olsson V, Anker MK, Albert M. 2018. The dynamics of root cap sloughing in Arabidopsis is regulated by peptide signalling. *Nature plants* **4**(8): 596-604.

Sierla M, Waszczak C, Vahisalu T, Kangasjarvi J. 2016. Reactive Oxygen Species in the Regul ation of Stomatal Movements. *Plant Physiol* **171**(3): 1569-1580.

Skubacz A, Daszkowska-Golec A, Szarejko L. 2016. The Role and Regulation of ABI5 (ABA-In sensitive 5) in Plant Development, Abiotic Stress Responses and Phytohormone Crosstal k. *Frontiers in Plant Science* **7** : 1884.

Smyth DR, Bowman JL, Meyerowitz EM. 1990. Early flower development in Arabidopsis. *The Plant Cell* **2**(8): 755-767.

Stenvik GE, Tandstad NM, Guo Y, Shi CL, Kristiansen W, Holmgren A, Clark SE, Aalen RB,

Butenko MA. 2008. The EPIP peptide of INFLORESCENCE DEFICIENT IN ABSCISSION is sufficient to induce abscission in Arabidopsis through the receptor-like kinases HAESA and HAESA-LIKE2. *Plant Cell* **20**(7): 1805-1817.

Straus MR, Rietz S, Ver Loren van Themaat E, Bartsch M, Parker JE. 2010. Salicylic acid antagonism of EDS1-driven cell death is important for immune and oxidative stress responses in Arabidopsis. *The Plant Journal* **62**(4): 628-640.

Tanaka T, Tanaka H, Machida C, Watanabe M, Machida Y. 2004. A new method for rapid visualization of defects in leaf cuticle reveals five intrinsic patterns of surface defects in Arabidopsis. *The Plant Journal* **37**(1): 139-146.

Taylor JE, Whitelaw CA. 2001. Signals in abscission. *New Phytologist* **151**(2): 323-340.

Tsukagoshi H, Busch W, Benfey PN. 2010. Transcriptional regulation of ROS controls transition from proliferation to differentiation in the root. *Cell* **143**(4): 606-616.

Tucker ML, Yang R. 2012. IDA-like gene expression in soybean and tomato leaf abscission and requirement for a diffusible stelar abscission signal. *AoB PLANTS* **2012**: pls035.

Ventimilla D, Domingo C, González-Ibeas D, Talon M, Tadeo FR. 2020. Differential expression of IDA (INFLORESCENCE DEFICIENT IN ABSCISSION)-like genes in Nicotiana benthamiana during corolla abscission, stem growth and water stress. *BMC plant biology* **20**(1): 1-14.

Ventimilla D, Velázquez K, Ruiz-Ruiz S, Terol J, Pérez-Amador MA, Vives MC, Guerri J, Talon M, Tadeo FR. 2021. IDA (INFLORESCENCE DEFICIENT IN ABSCISSION)-like peptides and HAE (HAESA)-like receptors regulate corolla abscission in Nicotiana benthamiana flowers. *BMC plant biology* **21**(1): 1-14.

Vie AK, Najafi J, Liu B, Winge P, Butenko MA, Hornslien KS, Kumpf R, Aalen RB, Bones AM, Brembu T. 2015. The IDA/IDA-LIKE and PIP/PIP-LIKE gene families in Arabidopsis: phylogenetic relationship, expression patterns, and transcriptional effect of the PIPL3 peptide. *Journal of Experimental Botany* **66**(17): 5351-5365.

Vierstra RD. 1993. Protein degradation in plants. *Annual review of plant biology* **44**(1): 385-410.

Vishwakarma A, Wany A, Pandey S, Bulle M, Kumari A, Kishorekumar R, Igamberdiev AU, Mur LAJ, Gupta KJ. 2019. Current approaches to measure nitric oxide in plants. *J Exp Bot* **70**(17): 4333-4343.

Wang L, Li Z, Wang C, Wang D, Wang Y, Lu M. 2017. Overexpression of a peroxiredoxin gene from Tamarix hispida, ThPrx1, confers tolerance to oxidative stress in yeast and Arabidopsis. *Journal of Plant Biology* **60**(6): 548-557.

Waszczak C, Carmody M, Kangasjarvi J. 2018. Reactive Oxygen Species in Plant Signaling. *Annu Rev Plant Biol* **69**: 209-236.

Xing Y, Cao Q, Zhang Q, Qin L, Jia W, Zhang J. 2013. MKK5 regulates high light-induced gene expression of Cu/Zn superoxide dismutase 1 and 2 in Arabidopsis. *Plant Cell Physiol* **54**(7): 1217-1227.

Yamasaki H, Abdel-Ghany SE, Cohu CM, Kobayashi Y, Shikanai T, Pilon M. 2007. Regulation of copper homeostasis by micro-RNA in Arabidopsis. *J Biol Chem* **282**(22): 16369-16378.

Yan M, Jing W, Xu N, Shen L, Zhang Q, Zhang W. 2016. Arabidopsis thaliana constitutively active ROP11 interacts with the NADPH oxidase respiratory burst oxidase homologue F to regulate reactive oxygen species production in root hairs. *Functional Plant Biology* **43**(3): 221-231.

Yang H, Kim HJ, Chen H, Lu Y, Lu X, Wang C, Zhou B. 2018. Reactive oxygen species and nitric oxide induce senescence of rudimentary leaves and the expression profiles of the related genes in Litchi chinensis. *Hortic Res* **5**: 23.

Yang ZQ, Zhong XM, Fan Y, Wang HC, Li JG, Huang XM. 2015. Burst of reactive oxygen species in pedicel-mediated fruit abscission after carbohydrate supply was cut off in longan (Dimocarpus longan). *Frontiers in Plant Science* **6**: 360.

Ye J, Zhang Y, Cui H, Liu J, Wu Y, Cheng Y, Xu H, Huang X, Li S, Zhou A, et al. 2018. WEGO 2.0: a web tool for analyzing and plotting GO annotations, 2018 update. *Nucleic Acids Research* **46**(W1): W71-W75.

Figure legends

Fig. 1. Floral organ abscission is accelerated in *msd2* Arabidopsis mutants. (a) Expression pattern of *MSD2*, as revealed by GUS staining using transgenic lines expressing *MSD2pro:nGFP-GUS* at the indicated flower stages. Yellow arrowheads indicate the GUS pattern in nectary (S16) and sepal, respectively. (b) Confocal microscopy showing the localization of MSD2-mCherry in residual cells (RECs) and secession cells (SECs) in Stage 16 (S16) flowers. Calcofluor white was used to reveal the cell wall and FM1-43 was used to stain the tonoplast. (c) Abscission phenotypes of the wild type (WT), *msd2-1* and *msd2-2* mutants and *msd2-1 UBQ10pro:MSD2-mCherry* transgenic plants (*msd2-1 MSD2ox*) in S16 flowers. (d, e) Quantification of abscission phenotypes as length of siliques extending above S16 flowers (d) and the position of S16 flowers (e). n = 30. (f) Permeability of the abscission zone (AZ), as visualised by toluidine blue (TB) staining. (g) Visualisation of superoxide anion accumulation using nitroblue tetrazolium (NBT) staining. Yellow arrowheads indicate the first flower showing permeable staining with TB (f, g). Different letters indicate significant differences ($P < 0.05$, one-way ANOVA with post-hoc Tukey test [d], and Kruskal-Wallis with Dunn's multiple comparison test [e]). P, flower position counted after anthesis (f, g). Bars, 200 μm (a), 50 μm (b; left panel), 5 μm (b; right panel) and 1 mm (c, f, g).

Fig. 2. The timing of *IDA* and *HAE* expression in the abscission zone (AZ) accelerates in the *msd2-1* Arabidopsis mutant. (a) Promoter analysis of *IDA* and *HAE* in the WT (Col-0) and the *msd2-1* mutant harbouring the reporter constructs *IDApro:GUS* and *HAEpro:GUS*. Yellow arrowheads indicate the first flower showing GUS pattern. (b) Relative expression levels of the indicated genes in the AZ of WT and *msd2-1* plants by floral position, as determined by RT-qPCR. *ACTIN2* served as a reference gene. Values represent means ± standard error of the means (SEM) of three independent experiments. Different letters indicate significant differences (n = 3; $P < 0.05$, one-way ANOVA with post-hoc Tukey test). (c) Abscission phenotype in the *hae hsl2* double mutant and the *hae hsl2 msd2-1* triple mutant. P, flower position counted after anthesis (a, c). Bars, 1 mm.

Fig. 3. Changes in gene expression in *msd2-1* assessed by RNA-seq. (a) Heatmap representation of Log_2-normalised counts per million across all samples for DEGs in the mutant relative to the wild type (WT). A cut-off probability P-value < 0.05, FDR < 0.05, and |Fold-change| ≥ 2 were applied to genes expressed in each sample. (b) Differentially expressed gene (DEG) counts among sets C13 vs m13 (control S13 vs *msd2-1* S13, bold), C15 vs m15 (control S15 vs *msd2-1* S15, bold), C13 vs C15, and m13 vs m15. (c) Venn diagram showing the overlap between DEG sets between C13 vs m13 (upper panel) and C15 vs m15 (lower panel). (d) GO term enrichment analysis. Web Gene Ontology Annotation Plot (WEGO) output for GO enrichment analysis for biological functions within the DEGs between C13 vs m13 and C15 vs m15 with adjusted P-value < 0.05. (e) Venn diagram (upper panel) and heatmap representation of expression levels of abscisic acid (ABA)-responsive DEGs between C13 vs C15 and C15 vs m15. (f) Venn diagram (upper panel) and heatmap representation of expression levels of nitric oxide (NO)-responsive DEGs between C13 vs C15 and C15 vs m15. (g) Heatmap representation of transcript levels for DEGs involved in ABA signalling pathways. In heatmaps, relative expression is scaled from red (high expression) to blue (low expression). Each column represents each replicate labelled 1 through 3, and each row represents a gene (a, d, e, f).

Fig. 4. Accelerated abscission in the *msd2-1* mutant is mediated by nitric oxide (NO). (a)

Confocal micrographs of the abscission zone (AZ) from a S15 flower stained with DAF-2DA. The NO scavenger cPTIO was applied to test specificity of DAF-2DA fluorescence for NO. (b) Quantification of DAF-2DA fluorescence intensity in the abscission zone (AZ) of wild type (WT) and *msd2-1* flowers in (a). n = 12. (c–e) Analysis of abscission after treatment with peroxynitrite ($ONOO^-$) and with or without 500 μM cPTIO. Drugs were mixed with lanolin wax and placed on the petioles of S13 flowers. Five days after treatment, permeability in the AZ was visualised by TB staining (c) and quantified by measuring the length of siliques extending over S16 flowers (d) and the position of S16 flowers (e). n = 12. (f–h) Analysis of abscission in the *msd2-1* mutant after treatment with cPTIO. Permeability of the AZ by toluidine blue (TB) staining (f), silique lengths extending above S16 flowers (g), and the position of S16 flowers (h) are shown. Different letters indicate significant differences. $P < 0.05$, one-way ANOVA with post-hoc Tukey test (b, d) and Kruskal-Wallis with Dunn's multiple comparisons test (e). $^{**}P < 0.01$; Student's *t*-test (g, h). P, flower position counted after anthesis (c, f). Bars, 100 μm (a) and 1 mm (c, f).

Fig. 5. The interaction of abscisic acid (ABA) with nitric oxide (NO) signalling is important for inducing abscission. (a) ABA contents in the abscission zone (AZ) from the wild type (WT) and *msd2-1* mutant. Values represent means ± SEM (n = 3). (b–d) Analysis of abscission in the WT after treatment with 50 μM ABA and with or without 500 μM cPTIO. Permeability of AZ by toluidine blue (TB) staining (b), silique lengths extending above S16 flowers (c) and the position of S16 flowers (d) are reported (n = 15). (e–g) Analysis of abscission in the *abi5-7* mutant. Permeability of AZ by TB staining (e), silique lengths extending above S16 flowers (f), and the position of S16 flowers (g) were analysed (n = 20). (h) Relative expression levels of the indicated genes in the S15 AZ of the WT and *msd2-1* mutant, as determined by RT-qPCR. *ACTIN2* served as a reference gene. Values represent means ± SEM of three independent experiments (n = 3). Different letters indicate significant differences ($P < 0.05$, one-way ANOVA with post-hoc Tukey test (a, c) and Kruskal-Wallis with Dunn's multiple comparisons test (d)). $^{*}P < 0.05$, $^{**}P < 0.01$; Student's *t*-test (f, g). P, flower position counted after anthesis (b, e). Yellow arrowheads indicate the first flower showing permeable staining with TB (b, e). Bars, 1 mm (b, e).

Fig. 6. Nitric oxide (NO) and abscisic acid (ABA) regulate abscission by modulating the expression of *IDA* and *HAESA*. (a-c) Analysis of abscission in *ida* (a-c) and *hae hsl2* (d) mutants 5 days after treatment with 50 μM ABA or 500 μM peroxynitrite ($ONOO^-$) in S13 flowers. Silique lengths extending above S16 flowers (b), the position of S16 flowers (c) in the *ida* mutant (n = 15). Yellow arrowheads indicate the first flower showing permeable staining with TB (a). (e) Relative expression levels of the indicated genes in S15 flowers of *ida* (upper panel) and *hae hsl2* (lower panel) mutants, as determined by RT-qPCR. Control values were set to 1 (n = 3). (f, g) Promoter activity analysis of *IDA* and *HAE* using the reporter lines *IDApro:GUS* (f) and *HAEpro:GUS* (g). Yellow arrowheads indicate the first flower showing GUS pattern. (h) Relative expression levels of *IDA* and *HAE* in S15 flowers after 5 days treatment with $ONOO^-$ or ABA, as determined by RT-qPCR. *ACT2* served as a reference gene. Control values were set to 1. Values represent means ± SEM of three independent experiments (n = 3). Different letters indicate significant differences (b, c, e, h; $P < 0.05$, one-way ANOVA with post-hoc Tukey test). P, flower position counted after anthesis (a, d, f, g). Bars, 1 mm (a, d, f, g).

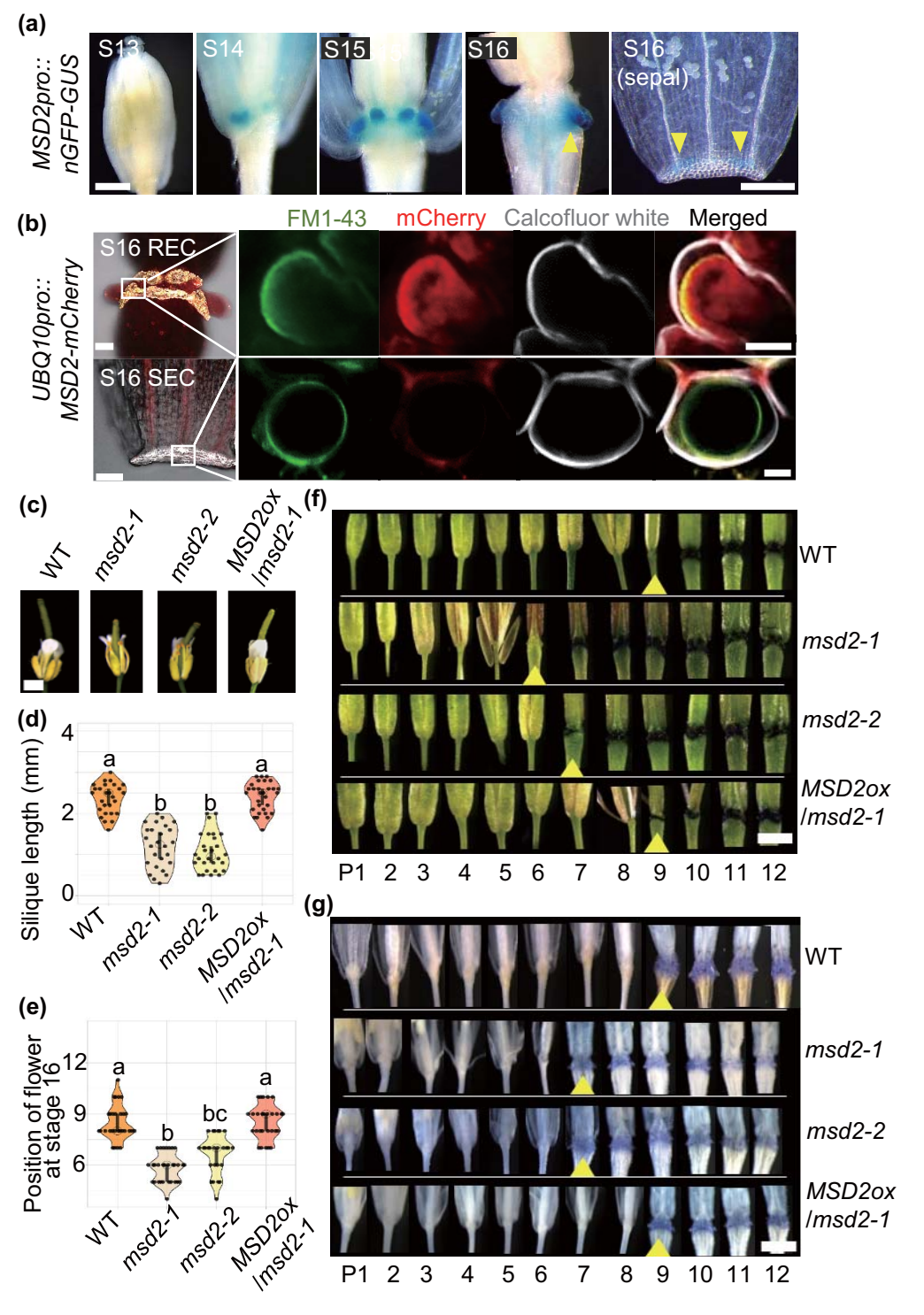
(a)
MSD2pro::
nGFP-GUS
S13
S14
S15
S16
S16
(sepal)
(b)
UBQ10pro::
MSD2-mCherry
FM1-43
mCherry
Calcofluor white
Merged
S16 REC
S16 SEC
(c)
WT
msd2-1
msd2-2
MSD2ox
/msd2-1
(d)
Silique length (mm)
4
2
0
a
b
b
a
WT
msd2-1
msd2-2
MSD2ox
/msd2-1
(e)
Position of flower
at stage 16
12
9
6
a
b
bc
a
WT
msd2-1
msd2-2
MSD2ox
/msd2-1
(f)
WT
msd2-1
msd2-2
MSD2ox
/msd2-1
P1 2 3 4 5 6 7 8 9 10 11 12
(g)
WT
msd2-1
msd2-2
MSD2ox
/msd2-1
P1 2 3 4 5 6 7 8 9 10 11 12

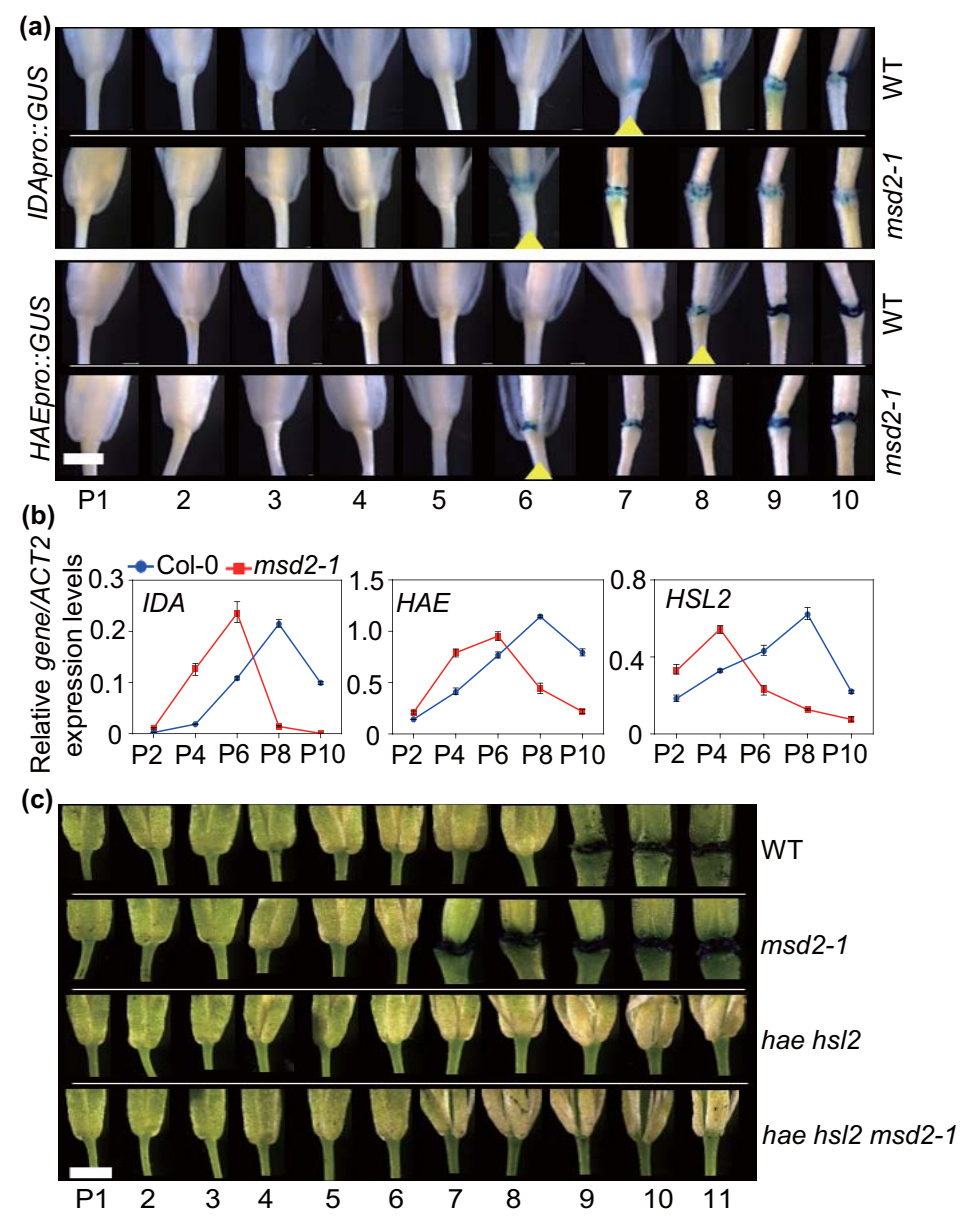
(a)
IDApro::GUS
WT
msd2-1
HAEpro::GUS
WT
msd2-1
P1 2 3 4 5 6 7 8 9 10
(b)
Relative gene/ACT2 expression levels
Col-0
msd2-1
IDA
HAE
HSL2
P2 P4 P6 P8 P10
(c)
WT
msd2-1
hae hsl2
hae hsl2 msd2-1
P1 2 3 4 5 6 7 8 9 10 11

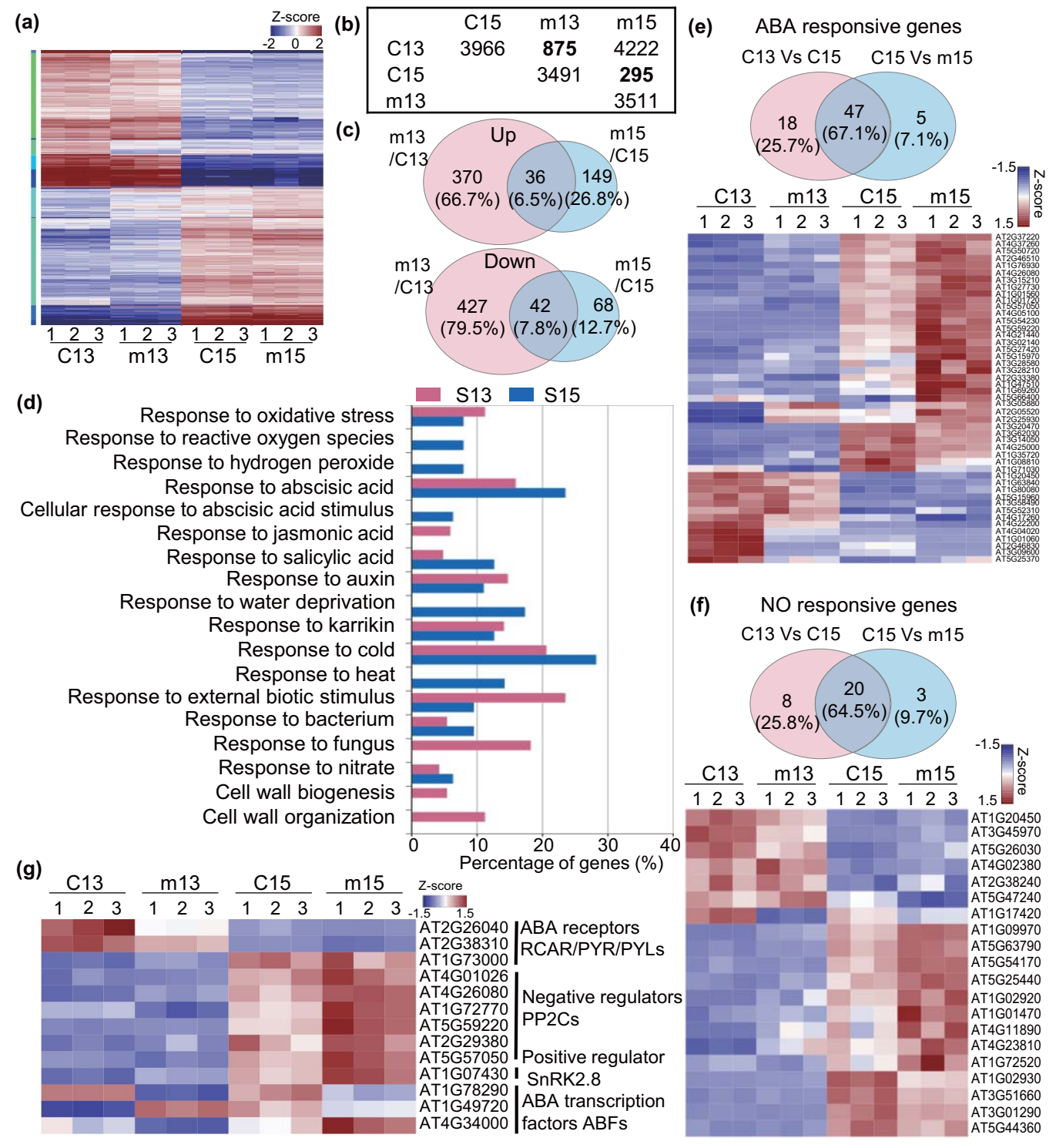
(a)
Z-score
-2 0 2
1 2 3 1 2 3 1 2 3 1 2 3
C13 m13 C15 m15
(b)
C15 m13 m15
C13 3966 875 4222
C15 3491 295
m13 3511
(c)
m13 /C13
Up
m15 /C15
370 (66.7%)
36 (6.5%)
149 (26.8%)
m13 /C13
Down
m15 /C15
427 (79.5%)
42 (7.8%)
68 (12.7%)
(d)
S13 S15
Response to oxidative stress
Response to reactive oxygen species
Response to hydrogen peroxide
Response to abscisic acid
Cellular response to abscisic acid stimulus
Response to jasmonic acid
Response to salicylic acid
Response to auxin
Response to water deprivation
Response to karrikin
Response to cold
Response to heat
Response to external biotic stimulus
Response to bacterium
Response to fungus
Response to nitrate
Cell wall biogenesis
Cell wall organization
0 10 20 30 40
Percentage of genes (%)
(e)
ABA responsive genes
C13 Vs C15
C15 Vs m15
18 (25.7%)
47 (67.1%)
5 (7.1%)
C13 m13 C15 m15
1 2 3 1 2 3 1 2 3 1 2 3
-1.5 1.5 Z-score
AT2G37220
AT4G37260
AT5G50720
AT2G46510
AT1G76930
AT4G26080
AT3G15210
AT1G27730
AT1G01560
AT1G01720
AT5G57050
AT4G05100
AT5G54230
AT5G59220
AT4G21440
AT3G02140
AT5G27420
AT5G18970
AT3G25580
AT3G28210
AT2G33380
AT1G74310
AT1G69260
AT5G66400
AT3G05880
AT2G05520
AT2G25930
AT3G20470
AT3G62030
AT3G14060
AT4G25000
AT1G35720
AT1G08810
AT1G71030
AT1G20450
AT1G63840
AT1G80080
AT5G18960
AT3G58960
AT5G52310
AT4G17260
AT4G22200
AT4G04020
AT1G01060
AT2G46830
AT3G09600
AT5G25370
(f)
NO responsive genes
C13 Vs C15
C15 Vs m15
8 (25.8%)
20 (64.5%)
3 (9.7%)
C13 m13 C15 m15
1 2 3 1 2 3 1 2 3 1 2 3
-1.5 1.5 Z-score
AT1G20450
AT3G45970
AT5G26030
AT4G02380
AT2G38240
AT5G47240
AT1G17420
AT1G09970
AT5G63790
AT5G54170
AT5G25440
AT1G02920
AT1G01470
AT4G11890
AT4G23810
AT1G72520
AT1G02930
AT3G51660
AT3G01290
AT5G44360
(g)
C13 m13 C15 m15
1 2 3 1 2 3 1 2 3 1 2 3
Z-score
-1.5 1.5
AT2G26040
AT2G38310
AT1G73000
AT4G01026
AT4G26080
AT1G72770
AT5G59220
AT2G29380
AT5G57050
AT1G07430
AT1G78290
AT1G49720
AT4G34000
ABA receptors
RCAR/PYR/PYLs
Negative regulators
PP2Cs
Positive regulator
SnRK2.8
ABA transcription
factors ABFs

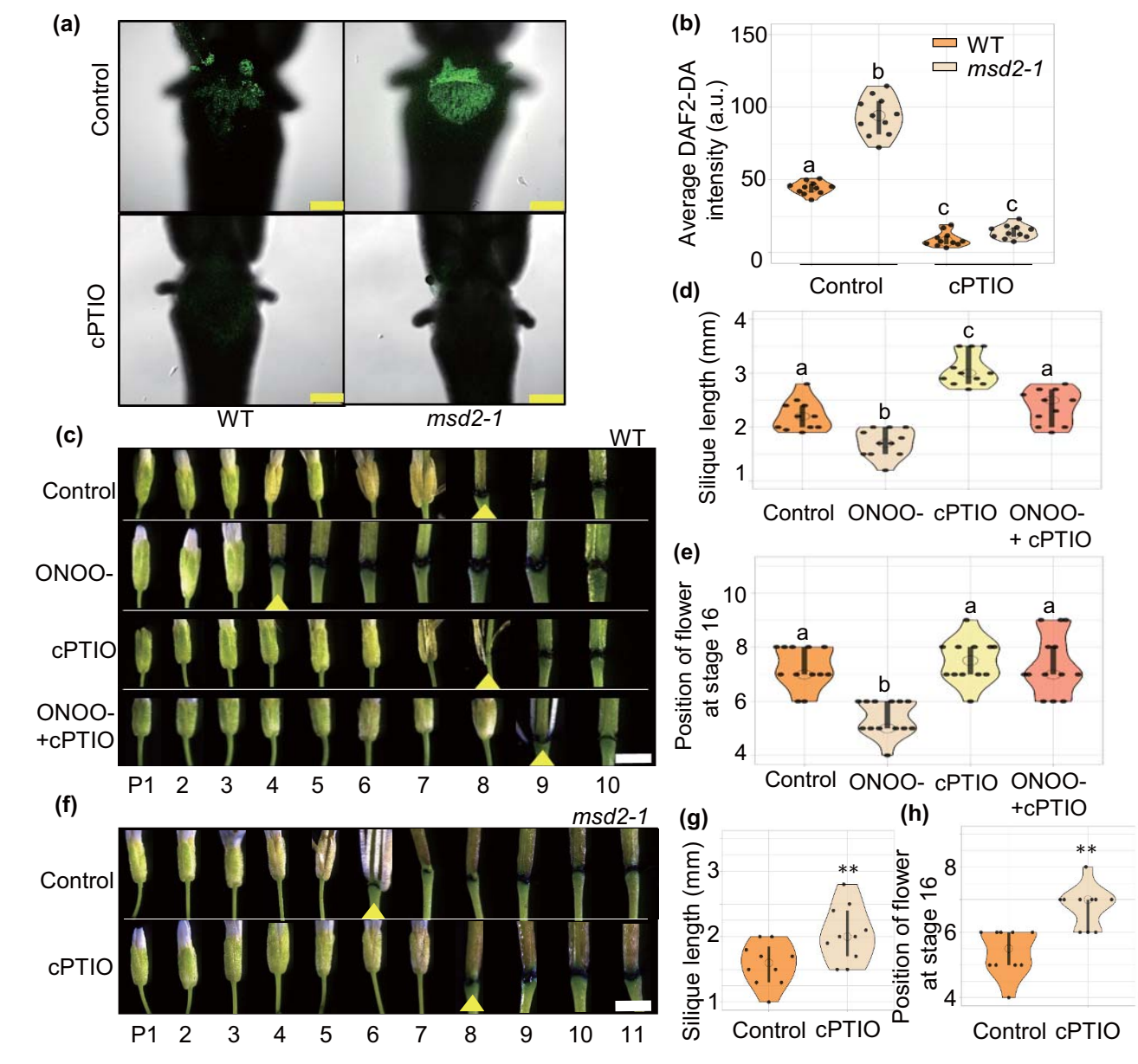
(a)
Control
cPTIO
WT
msd2-1
(b)
Average DAF2-DA intensity (a.u.)
150
100
50
0
WT
msd2-1
a
b
c
c
Control
cPTIO
(c)
WT
Control
ONOO-
cPTIO
ONOO- +cPTIO
P1 2 3 4 5 6 7 8 9 10
(d)
Silique length (mm)
4
3
2
1
a
b
c
a
Control
ONOO-
cPTIO
ONOO- + cPTIO
(e)
Position of flower at stage 16
10
8
6
4
a
b
a
a
Control
ONOO-
cPTIO
ONOO- +cPTIO
(f)
msd2-1
Control
cPTIO
P1 2 3 4 5 6 7 8 9 10 11
(g)
Silique length (mm)
3
2
1
**
Control
cPTIO
(h)
Position of flower at stage 16
8
6
4
**
Control
cPTIO

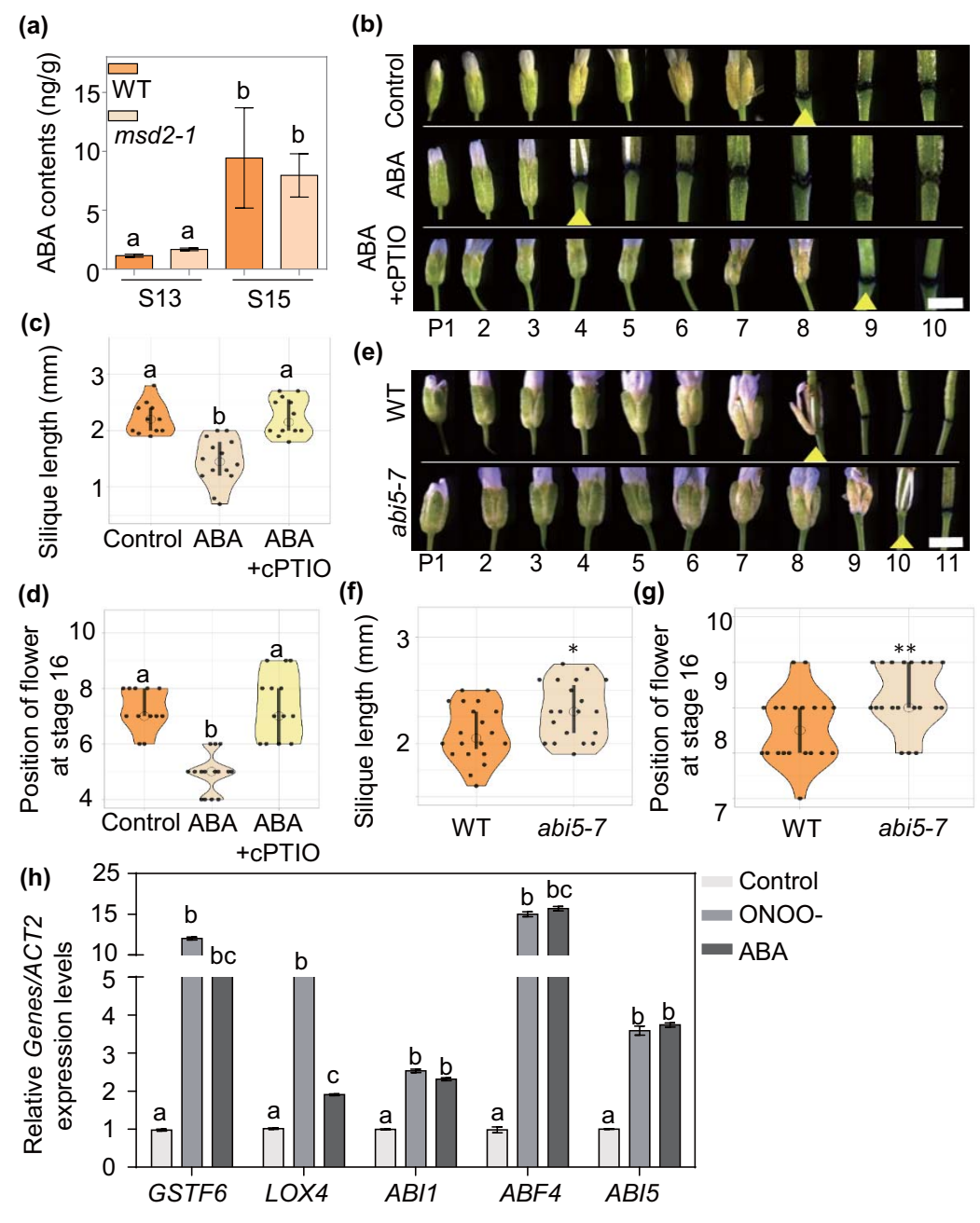
(a)
ABA contents (ng/g)
WT
msd2-1
S13
S15
(b)
Control
ABA
ABA +cPTIO
P1 2 3 4 5 6 7 8 9 10
(c)
Silique length (mm)
Control ABA ABA +cPTIO
(e)
WT
abi5-7
P1 2 3 4 5 6 7 8 9 10 11
(d)
Position of flower at stage 16
Control ABA ABA +cPTIO
(f)
Silique length (mm)
WT abi5-7
(g)
Position of flower at stage 16
WT abi5-7
(h)
Relative Genes/ACT2 expression levels
Control
ONOO-
ABA
GSTF6 LOX4 ABI1 ABF4 ABI5

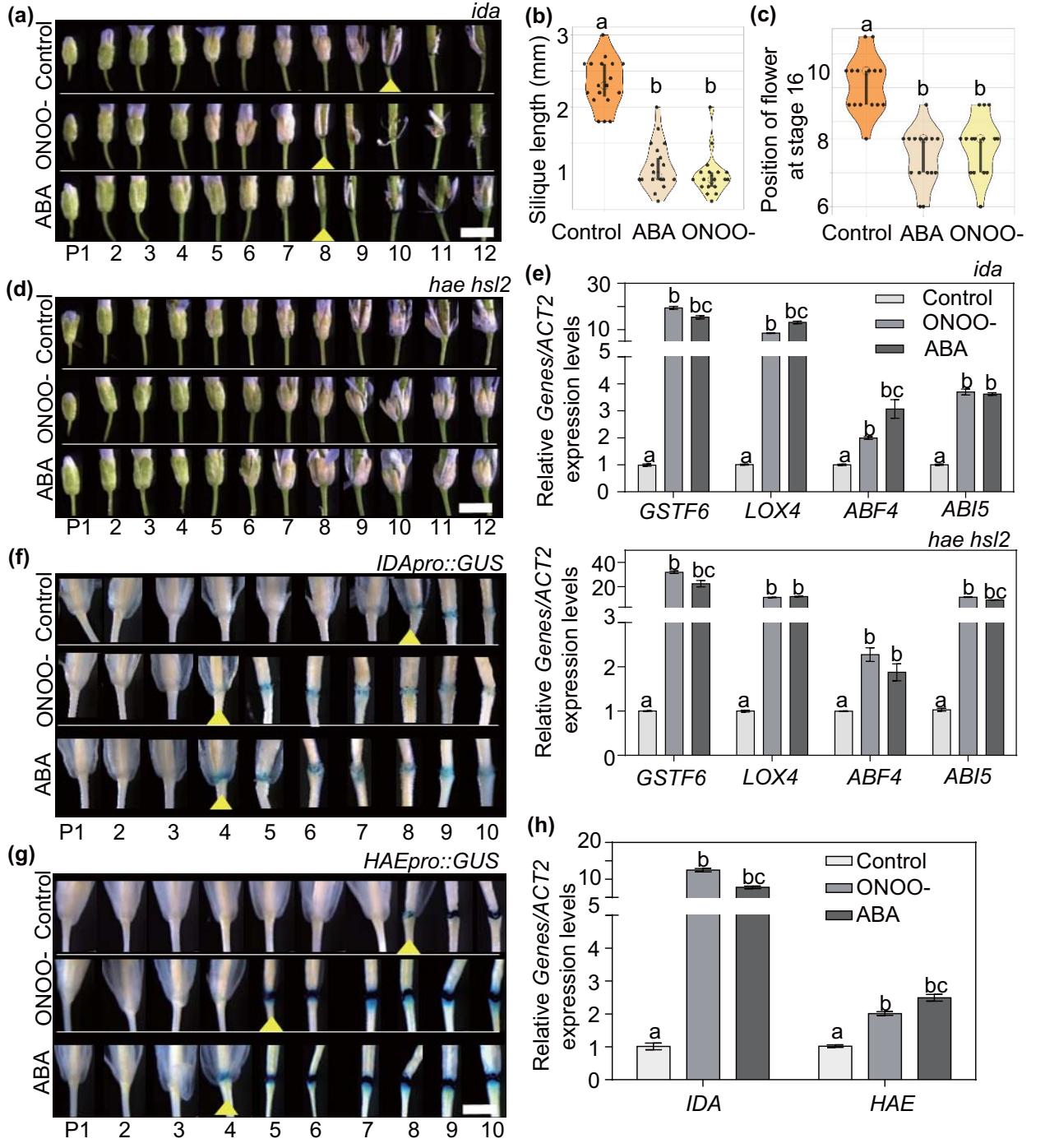
(a)
ida
Control
ONOO-
ABA
P1 2 3 4 5 6 7 8 9 10 11 12
(b)
Silique length (mm)
Control ABA ONOO-
(c)
Position of flower at stage 16
Control ABA ONOO-
(d)
hae hsl2
(e)
ida
Relative Genes/ACT2 expression levels
Control
ONOO-
ABA
GSTF6 LOX4 ABF4 ABI5
hae hsl2
(f)
IDApro::GUS
(g)
HAEpro::GUS
(h)
IDA HAE